RESEARCH ARTICLE

# Expression Pattern of Nogo-A, MAG, and NgR in Regenerating Urodele Spinal Cord

**Subhra Prakash Hui,[1] James R. Monaghan,[2] S. Randal Voss,[3] and Sukla Ghosh[1]***

**Background: The mammalian central nervous system is incapable of substantial axon regeneration after injury partially due to the presence of myelin-associated inhibitory molecules including Nogo-A and myelin associated glycoprotein (MAG). In contrast, axolotl salamanders are capable of considerable axon regrowth during spinal cord regeneration. Results: Here, we show that Nogo-A and MAG, and their receptor, Nogo receptor (NgR), are present in the axolotl genome and are broadly expressed in the central nervous system (CNS) during development, adulthood, and importantly, during regeneration. Furthermore, we show that Nogo-A and NgR are co-expressed in Sox2 positive neural progenitor cells. Conclusions: These expression patterns suggest myelin-associated proteins are permissive for neural development and regeneration in axolotls. *Developmental Dynamics 242:847–860, 2013*. © 2013 Wiley Periodicals, Inc.**

**Key words:** regeneration; axolotl; spinal cord injury (SCI); Nogo-A; Nogo receptor (NgR); myelin associated glycoprotein (MAG)

**Key Findings:**

- Myelin associated factors (MAFs) are expressed in axolotl spinal cord during development and adulthood.
- Both Nogo-A and NgR are expressed in neural progenitor cells during spinal cord regeneration.
- In contrast to mammals these MAFs are permissive for CNS development and regeneration in axolotl.

Accepted 28 March 2013

## INTRODUCTION

The failure of axon regeneration in the mammalian central nervous system (CNS) is partly due to the presence of myelin-associated inhibitory factors (MAFs) (Berry, 1982). The three MAFs present in mammalian CNS myelin are Nogo (Chen et al., 2000; Grandpre et al., 2000; Prinjha et al., 2000; Buchli and Schwab, 2005), myelin associated glycoprotein (MAG) (McKerracher et al., 1994), and oligodendrocyte-myelin glycoprotein (OMgp) (Kottis et al., 2002; Wang et al., 2002). These molecules impair neurite outgrowth in vitro and are thought to limit axonal growth in vivo after CNS injury (Schwab and Caroni, 1988; Caroni and Schwab, 1988) through binding to a common receptor, the Nogo-66 receptor (NgR) (Fournier et al., 2001; Wang et al., 2002; Domeniconi et al., 2002; Liu et al., 2002). Binding of MAFs to NgR induces intracellular signaling by means of activation of the neuronal GTPase RhoA, which regulates cytoskeletal dynamics and axonal outgrowth (McGee and Strittmatter, 2003; Burridge and Wennerberg, 2004). Due to their inhibitory properties, MAFs and their downstream signaling components are considered targets for treating CNS trauma (Buchli and Schwab, 2005; Freund et al., 2006). However, to gain more insight into the therapeutic potential of MAFs, we studied their expression during development and injury. So far, none of these molecules has been cloned in axolotl and little is known about patterns of expression and function in this regeneration competent species. Here, we describe the

Additional Supporting Information may be found in the online version of this article.

[1]Department of Biophysics, Molecular Biology and Bioinformatics, University of Calcutta, Kolkata, India
[2]Department of Biology, Northeastern University, Boston, Massachusetts
[3]Department of Biology, University of Kentucky, Lexington, Kentucky

Grant sponsor: Department of Science and Technology, Government of India; Grant number: SR/SO/AS-26/2004; Grant sponsor: Department of Biotechnology, Government of India; Grant number: DBT/BT/PR13953/AAQ/03/523/2010; Grant sponsor: Kentucky Spinal Cord and Brain Injury Research Trust; Grant sponsor: National Science Foundation.

Drs. Hui and Managhan contributed equally to this work.

***Correspondence to: Sukla Ghosh, Department of Biophysics, Molecular Biology and Bioinformatics, University of Calcutta, 92 A. P. C. Road, Kolkata −700009, India. E-mail: suklagh2010@gmail.com**

**DOI: 10.1002/dvdy.23976**
Published online 17 April 2013 in Wiley Online Library (wileyonlinelibrary.com).



Developmental Dynamics

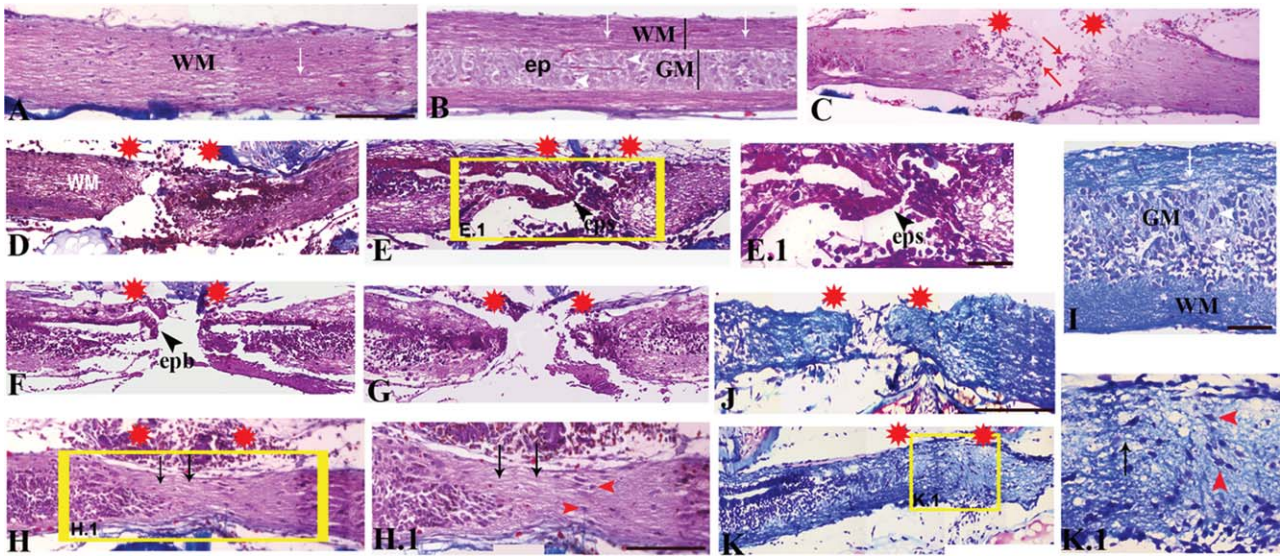


**Fig. 1.** Time course analysis of regeneration after transection injury of the adult axolotl spinal cord. Longitudinal sections of uninjured (A,B,I) and injured (C–H,K) axolotl spinal cord after trichrome (A–H) and luxol fast blue & cresyl violet (I–K) staining, respectively. **A,B,I:** Uninjured cord sections show the presence of white matter (WM) and constituent axons (white arrow), gray matter (GM) and compact ependyma (ep). **C:** A 3 days postinjury (dpi) section showing transected cord with loss of tissue and infiltration of red blood cells (red arrow) at the injury epicenter (double red star). **D,E:** Sections of 5 dpi cord showing separated stumps at the injury epicenter (double red star) and in a subsequent section, sealing of the ependymal canal (eps) is obvious. **E.1:** Same 5 dpi cord section at higher magnification showing sealed ependymal canal (eps). **F:** Section of 7 dpi cord shows formation of the ependymal bulb (epb). **G,J:** Two different sections of 7 dpi cord showing separate stumps with no axonal sparing. **H,H.1:** (Higher magnification of H): Section of 21 day regenerated cord showing axonal regrowth (black arrow) and cell bodies (red arrowheads) at the injury epicenter (double red star). **K:** 15 dpi cord showing regenerated axons at the injury epicenter (double red star). **K.1:** Higher magnification showing both regenerating axon (black arrow) and cell bodies (red arrowheads) at the injury site. Scale bar = 300 μm in A–H,K, 100 μm in H.1,J, 50 μm in E.1,I,K.1.

cloning of *nogo-A* and expression analyses of Nogo-A, NgR, and MAG.

In contrast to mammals, some teleost fish and amphibians can substantially regenerate axons after spinal cord injury (SCI), apparently performing this task by circumventing the inhibitory factors found in mammals. Studies have shown that goldfish and axolotl CNS myelin are permissive substrates for mammalian axon growth and do not induce growth cone collapse, suggesting that fish and axolotls do not express MAFs in their CNS (Bastmeyer et al., 1991; Lang et al., 1995; Ankerhold et al., 1998). Recent work has demonstrated that *nogo* (Shypitsyna et al., 2011), *mag*, *omgp* (Bradford et al., 2011) and *ngr* (Klinger et al., 2004) are present in the zebrafish genome, another regeneration competent species capable of axon regeneration. The mammalian *nogo* gene is unique among MAFs because it codes for a long isoform termed Nogo-A, which contains two axon outgrowth inhibitory domains (Grandpre et al., 2000; Oertle et al., 2003). Of interest, this isoform has recently been discovered in zebrafish, so it is not the presence or absence of MAFs that determines regenerative ability (Shypitsyna et al., 2011). Here, we corroborate these results by identifying *nogo*, *mag*, *omgp*, and *ngr* in the axolotl. We also investigated Nogo-A, MAG, and NgR expression in the embryonic and adult axolotl CNS, and after SCI. We show that MAFs and NgR are broadly expressed in the CNS during development and regeneration, which suggests they may have important functional roles beyond inhibition of axon outgrowth.

## RESULTS

### Time Course Analysis of Axonal Regrowth After Injury

To evaluate the extent of axonal regeneration in axolotl spinal cord, cords were transected and tissues were collected at several time points after injury (Fig. 1). Histological staining using trichrome (Fig. 1A–H) and luxol fast blue/cresyl violet (Fig. 1I–K) showed the presence of white matter, axonal fibers, oligodendrocyte cell bodies, and gray matter in uninjured (Fig. 1A,B,I) and injured cord (Fig. 1C-H,J-K). The gray matter was composed of a compact layer of ependyma that surrounded the ependymal canal (not shown), as well as neurons located in the subependyma (Fig. 1B,I). Neurons were identified in the gray matter by staining with the neuronal marker, NeuN (Fig. 2D). At 3 days postinjury (dpi), red blood cells (RBCs) were observed within the injury site, the ependymal canal was disrupted, and there was a substantial loss of white and gray matter tissue (Fig. 1C). Complete spinal cord transection was confirmed because two separate stumps were clearly observed in histological sections and no spared axons were seen at 3 dpi (Fig. 1C). The ependymal canal was sealed in 5 dpi cords (Fig. 1E) and ependymal bulb formation was observed in 7 dpi cords, when the two separate stumps were still recognizable (Fig. 1F,G,J). As time progressed, white and gray matter regeneration occurred simultaneously. Axonal regeneration was observed at the injury epicenter at 15 dpi (Fig. 1K,K.1), 21 dpi (Fig. 1H,H.1), and 30 dpi (data not shown), and the regeneration of neurons was also evident in the injury epicenter (Fig. 1H.1,K.1). Although regeneration was substantial, we note that the

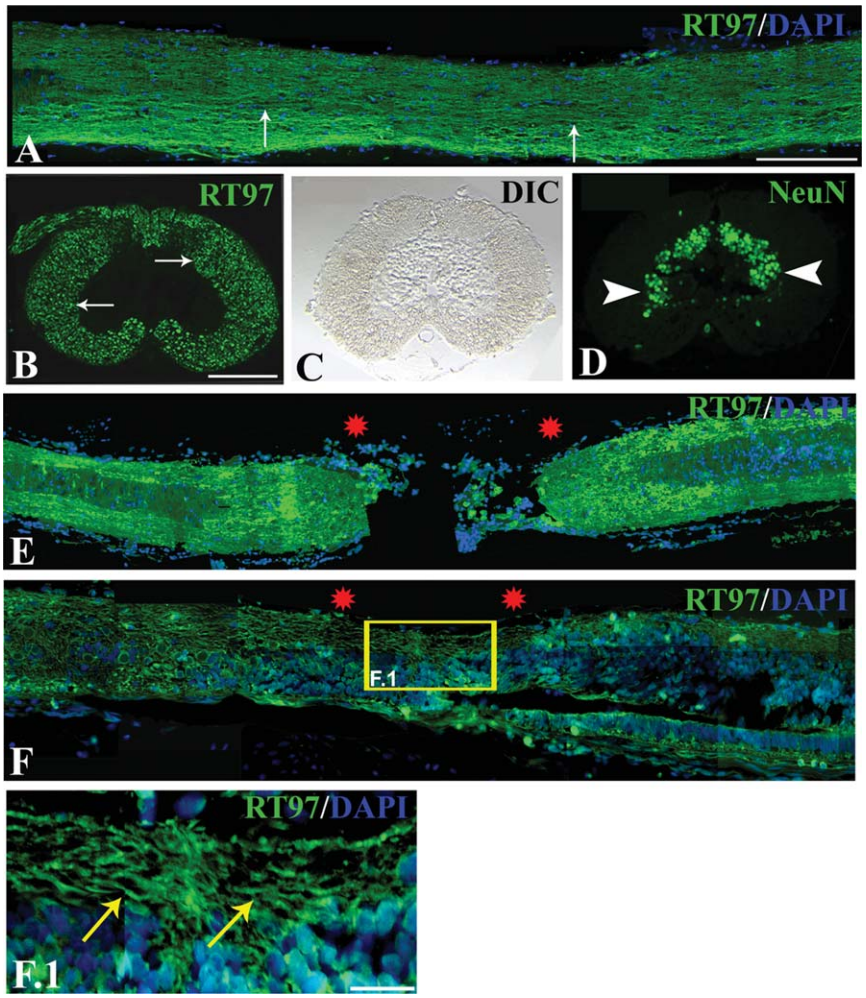


**Fig. 2.** RT-97 expression in uninjured and injured cord to show axonal regrowth after injury in adult axolotl spinal cord. Longitudinal sections of uninjured and injured cord stained with axonal marker RT-97. **A:** Section of uninjured cord showing axonal distribution (white arrow) in white matter as stained by RT-97 and counterstained with DAPI. **B:** A cross-section of uninjured cord showing normal distribution of axons (white arrow) in white matter. **C:** Differential interference contrast (DIC) image of B. **D:** Adjacent section of the same cord as in B stained with neuronal marker NeuN to show relative position of the neurons in the gray matter (white arrowheads). **E:** A 7 days post-injury (dpi) cord section showing RT-97 staining in the two stumps at the injury epicenter (double red star). **F:** Section of a 21 day regenerating cord showing presence of axons in normal part of the cord and reappearance of axonal fibers in the white matter of the injury site (double red star). **F.1:** Same cord at higher magnification showing regenerated axons (yellow arrow) in the injury site. Scale bar = 300 μm in A,E,F, 100 μm in B,C,D, 50 μm F.1.

volume of white matter was less than uninjured cords at 15, 21, and 30 dpi.

## Expression of RT-97 in Uninjured and Injured Cord

To further characterize axonal changes after transection injury, we stained uninjured and injured spinal cords using an antibody, RT-97 that recognizes neurofilament. In uninjured spinal cords, axons were distributed throughout the white matter (Fig. 2A,B). At 7 dpi, RT-97 expression was observed in the white matter, extending from the rostral and caudal stumps into uninjured regions of the severed cord (Fig. 2E). At 21 dpi (Fig. 2F,F.1) and 30 dpi (data not shown), expression of RT-97 was seen within the injury epicenter, suggesting axonal regeneration following SCI.

## Identification of *NOGO-A*, *MAG*, *OMGP*, and *RTN4R*

To establish that axolotls have orthologous axolotl sequences for *nogo*, *mag*, *omgp*, and *rtn4r* (gene encodes for NgR protein); groups of overlapping expressed sequence tags (isotigs) with sequence identity to MAFs were collected from Sal-Site (www.ambystoma.org). Blastx searches using isotigs as query sequences revealed high similarity to presumptive human orthologs (Supp. Table S1, which is available online). Furthermore, reciprocal blast searches of human MAFs to the axolotl database identified the same isotigs, strongly suggesting that all three MAFs and their receptor *rtn4r* are present in the axolotl.

Considering that the long Nogo-A protein isoform has been suggested to be absent in some lower vertebrates (Diekmann et al., 2005), we present additional evidence to establish that axolotl *nogo* (*axNogo*) is orthologous to amniote *nogo-a*. *axNogo* was genetically mapped to conserved synteny block 69 on linkage group 13 (LG13) of the *Ambystoma* genetic map (Voss et al., 2011). Eleven orthologous axolotl-chicken genes in this conserved synteny block, including *axNogo*, establishes that *axNogo* corresponds to amniote *nogo*. Overall, the presence of *nogo-a* in urodeles, anurans (Klinger et al., 2004), and bony fish (Shypitsyna et al., 2011) indicate that its origin dates to early-jawed vertebrates. Clearly, it is not the presence or absence of the MAFs in the genomes of these animals that determines regenerative ability.

## Comparison of Vertebrate Nogo-A Protein Sequences

To gain comparative insight about Nogo-A protein structure, we performed more complete sequence comparisons between axolotl Nogo-A and other vertebrate Nogo-A proteins. Protein alignments showed that the highest similarity between vertebrate Nogo proteins occurs within the reticulon homology domain (RHD) located at the carboxyl terminus (Fig. 3A). The axolotl RHD is 87% similar to the corresponding region in rat Nogo-A; only 34% of the non-RDH sequences are similar across the rest of the protein. The RHD contains two ~34 amino acid (aa) predicted transmembrane domains surrounding a 66 aa extracellular domain (Nogo-66; boxed area in 3A) that is thought to inhibit neurite outgrowth through binding to Nogo receptor (Fournier et al., 2001). The ~800 aa Nogo-A specific region is

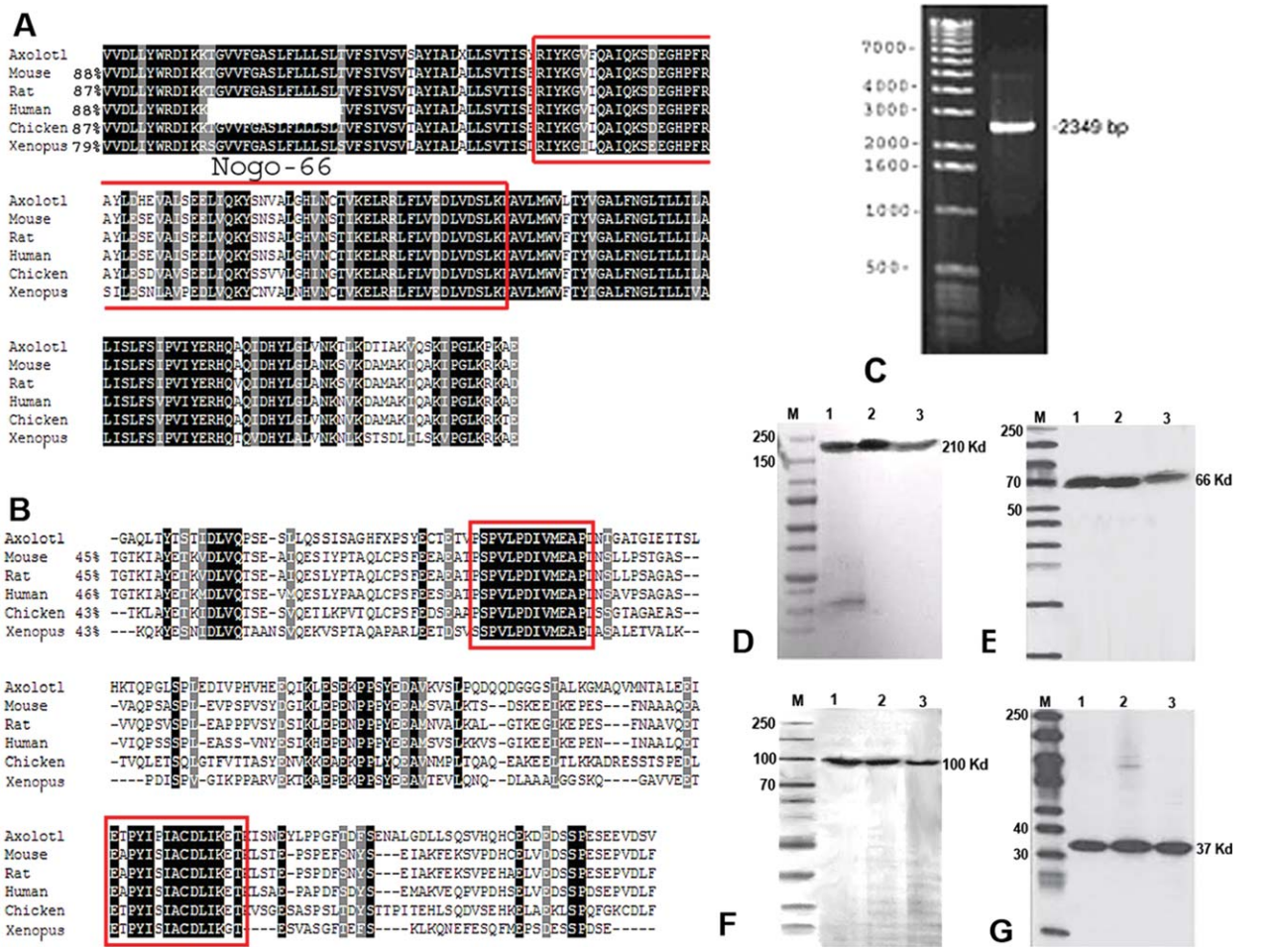


**Fig. 3.** Protein alignments of tetrapod Nogo-A. **A:** Predicted protein sequence alignment of the highly conserved carboxyl end of Nogo-A charactistic of all reticulon proteins. The red box indicates the Nogo-66 domain. **B:** Predicted protein sequence alignment of the Δ20 inhibitory domain located in the Nogo-A-specific region of the protein. Black shading represents 100% homology and gray shading representing similar amino acids. The red boxes indicate the known inhibitory regions within mammalian Nogo-A. **C:** Gel electrophoresis of the nested reverse transcriptase polymerase chain reaction product as produced using appropriate forward and reverse primers. **D–F:** Western blot analysis of Nogo-A, Nogo receptor (NgR), myelin associated glycoprotein (MAG) proteins respectively in axolotl uninjured tail and tail blastema. M = PageRuler Broad Range Protein Ladder (Thermo Scientific, USA), 1 = uninjured tail, 2 = 7 day tail blastema, 3 = 15 day tail blastema. **G:** GAPDH (glyceraldehyde-3-phosphate dehydrogenase) was used as control.

more divergent with similarity ranging from 32 to 36% between all vertebrates analyzed. A highly inhibitory region found within the rat Nogo-A specific region termed Δ20 (Oertle et al., 2003) shows higher similarity (45%) between rat and axolotl compared with the entire Nogo-A specific region (34%) (Fig. 3B). Overall, the regions responsible for inhibitory properties in mammals are more highly conserved in axolotls than the rest of the protein, suggesting conservation of function.

## Expression of Nogo-A and NgR

Expression of Nogo-A and its receptor NgR were evaluated at the transcript and protein levels. Reverse transcriptase polymerase chain reaction (RT-PCR) analysis showed that *nogo-a* and *rtn4r* transcripts were abundant in the nervous system including the eye, brain, and spinal cord (Figs. 4A, 5A). In situ hybridization localized *nogo-a* transcripts in gray matter neurons and cells in the white matter of the brain (Fig. 4B,C), and in the spinal cord (Fig. 4D,E). RT-PCR also showed that *nogo-a* and *rtn4r* transcript levels did not significantly change during spinal cord regeneration (Figs. 4G, 5B).

Similar results were observed at the protein level. Immunohistochemistry identified Nogo-A and NgR protein in the cerebellum, tectum, (Figs. 4F,4F.1; Fig. 5C,5C.1), and spinal cord (Figs. 4H-L, 5D-H). Western blot analysis demonstrated that the anti-Nogo-A and anti-NgR antibodies specifically recognized their targets and that each protein was expressed in uninjured tails (presumably spinal cords) as well as tail blastemas at 7 and 15 dpi (Fig. 3D,E). Immunohistochemistry was used to localize expression to white matter glia, white matter axons, and gray matter neurons of uninjured spinal cords (Figs. 4I,4I.1, Fig. 5E,5E.1; Supp. Fig. S2B) at 3 dpi (Figs. 4J-L.2, 5F-F.2,H,H.1), 7 dpi (Fig. 5G,G.1), and 15 dpi cord (data not shown). Specifically, Nogo-A was present in the axons, neurons (Fig. 4J,J.1,J.2,L; Supp. Fig. S2C), and cells near sub-pial membranes (Fig. 4J). To confirm neuronal

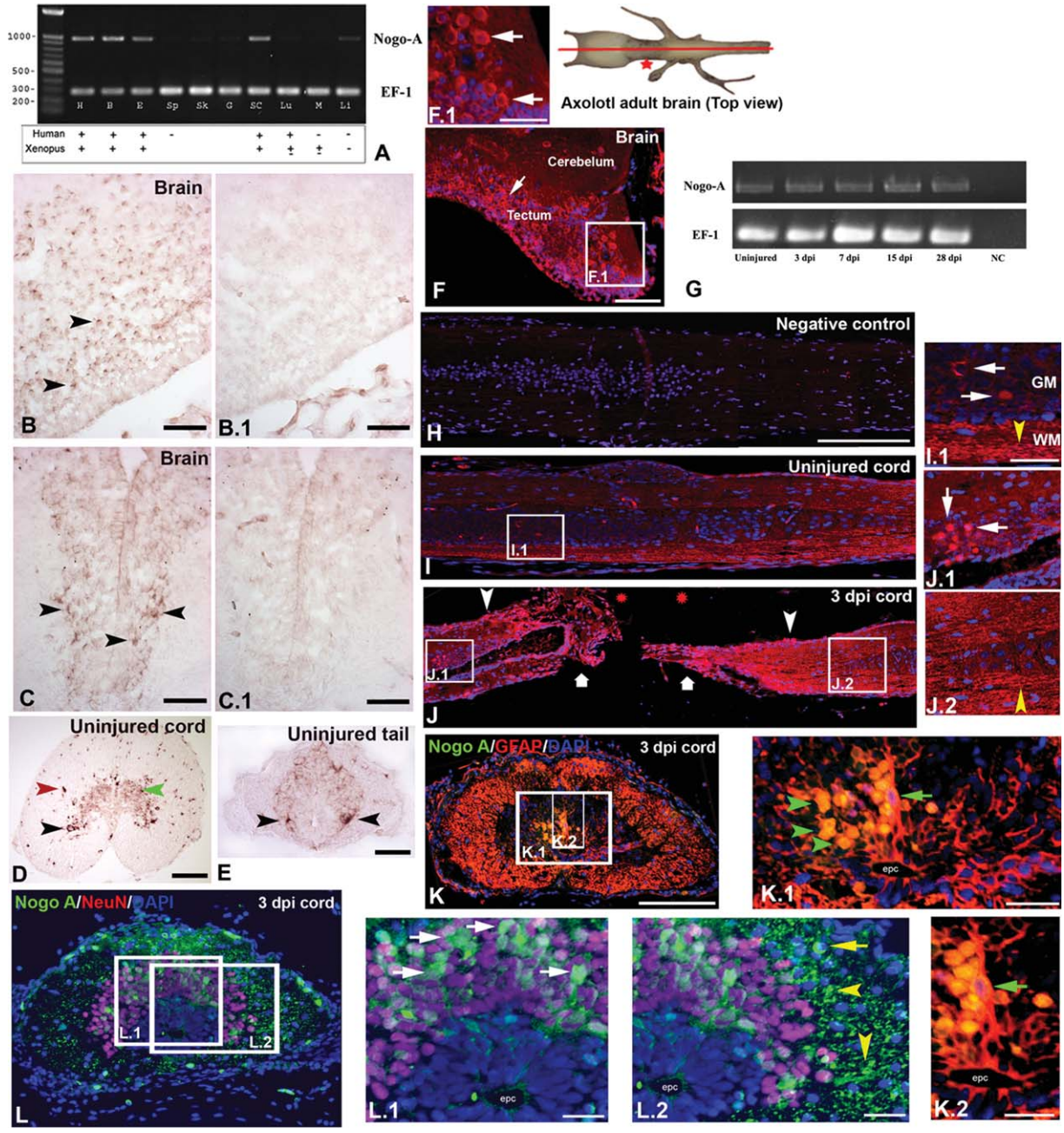


**Fig. 4.** Expression of Nogo-A in adult axolotl brain, uninjured cord and injured cord. **A:** Reverse transcriptase polymerase chain reaction (RT-PCR) of *nogo-a* in axolotl tissues compared with expression in adult human and *X. laevis* tissues. The top band is the specific *nogo-a* PCR product. The bottom band is the control *EF-1*$\alpha$ PCR product. The plus (+) and minus (–) indicate expression in humans and *X. laevis* modified from Klinger et al. (2004). H, heart; B, brain; E, eye; Sp, spleen; Sk, skin; G, gill; SC, spinal cord; Lu, lung; M, muscle; Li, liver. **B,B.1:** Representative antisense and sense *nogo-a* probe staining (black arrowhead) in the medial pallium region of axolotl brain, respectively. **C,C.1:** Representative antisense and sense *nogo-a* probe staining (black arrowhead) in the section of optic tectum region of axolotl brain, respectively. Note strong staining in the gray matter, within presumptive neurons. **D:** Both gray matter (black arrowhead) and white matter (red arrowhead) regions of the adult axolotl spinal cord show presence of *nogo-a* transcript. Ventral (black arrowhead) and dorsal (green arrowhead) neurons are both *nogo-a* positive. A few *nogo-a* positive cells in the white matter (red arrowhead) are likely oligodendrocytes. **E:** Presence of *nogo-a* transcript in an uninjured tail section. Staining is present in neurons, with strongest staining in the location of ventral neurons (black arrowhead). **F:** Immunohistochemical staining of Nogo-a antibody in a sagittal section of the midbrain, passing through the cerebellum. **F.1:** Same section showing Nogo-A positive neuronal cells in higher magnification in tectum. **G:** RT-PCR showing relative amounts of *nogo-A* mRNA in uninjured and injured cord at different time points (3, 7, 15, and 28 days post-injury [dpi]). *Ef-1*$\alpha$ was used as a reference gene. NC represents no RNA control. **H:** Longitudinal section of uninjured cord stained without Nogo-A primary antibody represented as negative control. **I:** Immunohistochemical staining of Nogo-A in a longitudinal section of uninjured cord. **I.1:** Higher magnification of the same cord where Nogo-A staining is found both in gray matter (GM) neurons (white arrow) and white matter (WM) axons (yellow arrowhead) of the cord. **J:** Immunohistochemical staining of Nogo-A antibody in a 3 dpi cord section shows many Nogo-A positive cells in the stump (thick arrow); few Nogo-A positive cells are near the sub-pial membrane (white arrowheads) in the adjacent part of the injury epicenter (double red star). **J.1,J.2**: Higher magnifications of the same 3 dpi cord showing positive staining in neurons (white arrow) and axons (yellow arrowhead). **K**: A transverse section of 3 dpi cord through the region immediately adjacent to the injury epicenter, stained with Nogo-A and glial fibrillary acidic protein (GFAP). **K.1,K.2**: Higher magnifications of the boxed area in same section (K) showing many Nogo-A and GFAP colocalized cells (green arrowheads) in the sub-ependyma and few around the ependymal canal (epc, green arrow) which may resemble radial glia. **L**: A transverse section of 3dpi cord at the stump level stained with Nogo-A and NeuN. **L.1,L.2**: Higher magnifications of boxed area (L) showing many Nogo-A and NeuN colocalized cells in the gray matter (white arrow) of the cord. Note that axonal cut ends (yellow arrowheads) and white matter cells (yellow arrow) are Nogo-A positive. The cartoon of axolotl brain (top view) has been adapted from the Eisthen lab (Michigan State University, USA) to show the plane of section and region of the brain as represented in sections stained with Nogo-A antibody. Scale bar = 300 $\mu$m in H–J; 100 $\mu$m in K,L; 50 $\mu$m in B–F,B.1,C.1; 20 $\mu$m in F.1,I.1,J.1,J.2,K.1,L.1,L.2; 10 $\mu$m in K.2).

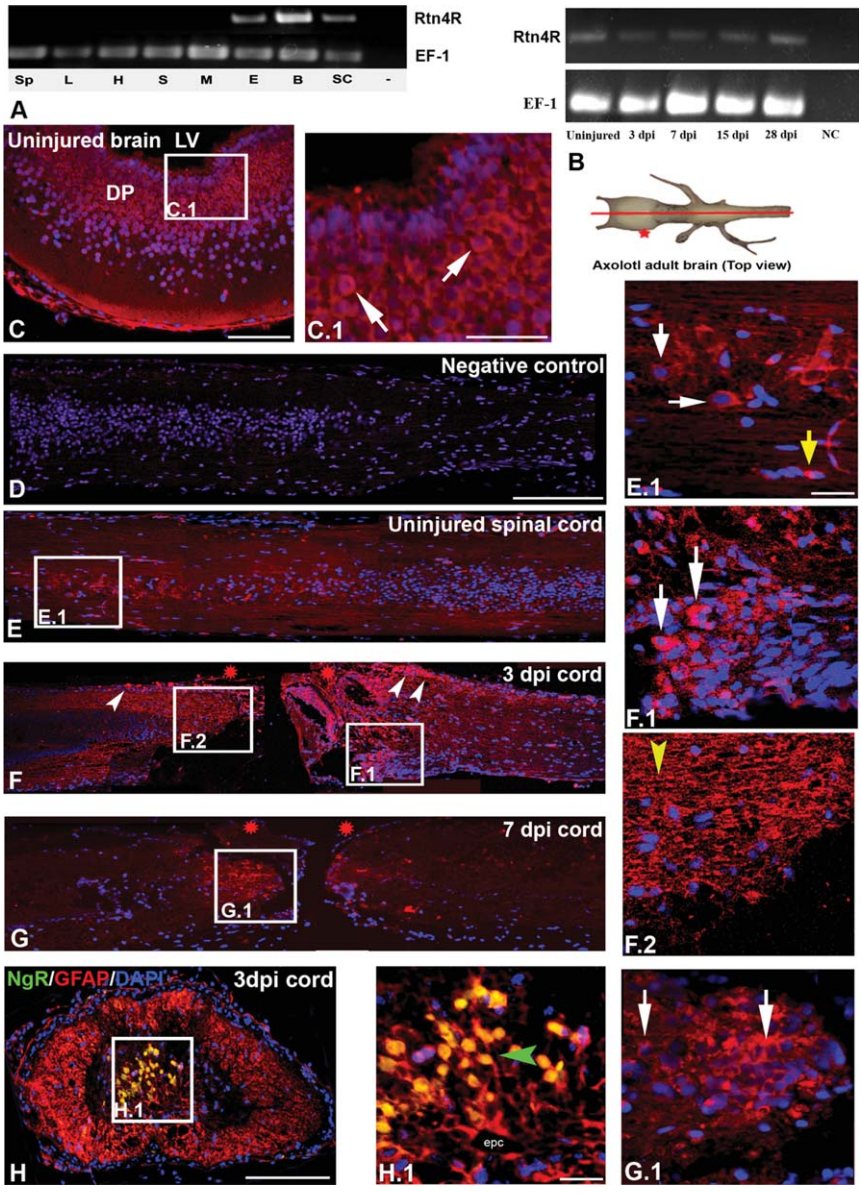


**Fig. 5.** Expression of Nogo receptor (NgR) in adult axolotl brain, uninjured and injured cord. **A:** Reverse transcriptase polymerase chain reaction (RT-PCR) of *Rtn4R* and *ef1α* in axolotl tissues. Sp = spleen, L = liver, H = heart, S = skin, M = muscle, E = eye, B = brain, SC = spinal cord. **B:** RT-PCR showing relative amounts of *Rtn4R* mRNA in uninjured and injured cord with different time points (3, 7, 15, and 28 days post-injury [dpi]). *Ef1α* was used as a reference gene. NC represents no RNA control. **C:** Sagittal section of forebrain through the lateral ventricle, showing immunohistochemical staining of NgR. **C.1:** In higher magnifications, the same section (C) shows NgR positive neurons of the dorsal pallium (DP), close to the lateral ventricle (LV). **D:** Longitudinal section of uninjured cord stained without NgR primary antibody; a negative control. **E:** Longitudinal section of uninjured cord stained with NgR antibody. **E.1:** Higher magnification of the same section (E) showing many NgR positive neuronal cells (white arrow) in the gray matter and fewer cells (presumably oligodendrocytes) in the white matter (yellow arrow). **F:** Longitudinal section of 3 dpi cord showing high level of NgR expression in the stump. Note that few cells near the sub-pial membrane (white arrowheads) at the injury epicenter (double red star) are NgR positive. **F.1,F.2:** Higher magnification of the same section (F) showing strong staining of neurons (white arrow) and of axons (yellow arrowhead) in the injury epicenter (double red star). **G:** 7 dpi cord section shows moderate staining of NgR at the stump. **G.1:** The same section (G) in higher magnification. **H:** A transverse section through the stump of 3 dpi cord shows NgR and glial fibrillary acidic protein (GFAP) staining. **H.1:** Higher magnification of the boxed area in the same section shows many NgR and GFAP colocalized cells (green arrowheads) in the sub-ependyma and fewer around the ependyma. The cartoon of axolotl brain (top view) was adapted from the Eisthen lab (Michigan State University, USA) to show the plane and region of the brain as represented in the section. Scale bar = 300 μm in D–G, 100 μm in H, 50 μm in C, 20 μm in C.1,E.1,F.1,F.2,G.1,H.1.

expression, Nogo-A was shown to colocalize with the neuronal marker NeuN in 3 dpi cords (Fig. 4L–L.2). Approximately 60% of the NeuN positive cells were also Nogo-A positive, as determined from differential counts in 3 dpi cord sections (data not shown). Nogo-A immunostaining also decreased farther away from the injury epicenter (Fig. 4J, Supp. Fig. S2). NgR showed similar expression patterns within 3 dpi cords, with strong expression observed among gray matter neurons (Fig. 5F,F.1; Supp. Fig. S3) and white matter axons (Fig. 5F,F.2; Supp. Fig. S3). A population of Nogo-A positive cells (approximately 50%) also showed NgR staining (Supp. Fig. S6). Both Nogo-A and NgR expression can be observed before and after injury, corroborating our RT-PCR and Western blot data that Nogo-A and NgR are expressed in the CNS before and during spinal cord regeneration. Lastly, we surprisingly found that some Nogo-A and NgR positive cells in the ependymal and sub-ependymal region colocalized with the glial marker, glial fibrillary acidic protein (GFAP; Figs. 4K–K.2, Fig. 5H,H.1); some of the cells have morphologies consistent with radial glia.

## Expression of MAG in Adult Axolotl Brain, and Uninjured and Injured Spinal Cord

The expression of MAG protein was characterized for injured and uninjured CNS tissues and compared with expression patterns of other MAFs. Western blot analysis showed that anti-MAG antibody specifically binds to axolotl MAG and is expressed before and after injury (Fig. 3F). Immunohistochemistry localized MAG protein to axons and neurons in the adult brain, especially at the brain stem-spinal cord junction (Fig. 6B,B.1), as well as uninjured cords (Fig. 6C,C.1). At 3 dpi, MAG protein was observed in cells and axons near the injury epicenter (Fig. 6D,D.1). The white matter of both immediate adjacent regions and regions distant from the injury epicenter also showed MAG positive axons (Supp. Fig. S4). There were also several cells near the sub-pial membrane of the injured

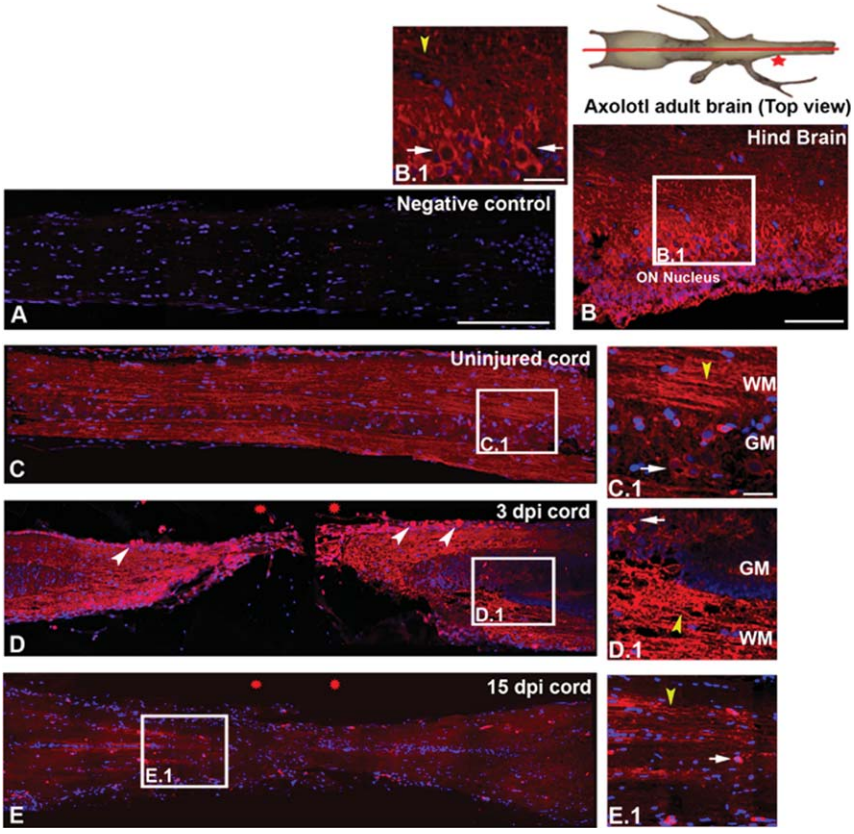


**Fig. 6.** Expression of myelin associated glycoprotein (MAG) in axolotl adult brain, uninjured and injured cord. **A:** Longitudinal section of uninjured cord stained without MAG primary antibody; a negative control. **B:** Sagittal section of hindbrain through the brain stem-spinal cord junction shows MAG staining. **B.1:** Same section in higher magnification showing MAG positive axons (yellow arrowhead) and octavo-lateralis neurons (white arrow). **C:** Longitudinal section of uninjured cord shows staining of MAG in gray and white matter. **C.1:** Higher magnification of the same section (C) shows strong staining in white matter (WM) axons (yellow arrowhead). Note that few gray matter (GM) cells (white arrow) are MAG positive. **D:** A 3 days post-injury (dpi) cord section shows strong MAG staining in the stump tissue and few cells near the sub-pial membrane (white arrowheads). **D.1** Higher magnification shows strong staining in white matter (WM) axons, (yellow arrowhead) and moderate staining of gray matter (GM) cells (white arrow) close to the injury epicenter (double red star). **E:** A 15 dpi cord section shows weak staining of MAG in the white matter just adjacent to the injury epicenter (double red star). **E.1:** Higher magnification of the boxed area (E) shows staining of MAG in axon (yellow arrowhead) and white matter cells (white arrow). The cartoon of the axolotl brain (top view) was adapted from the Eisthen lab, (Michigan State University, USA) to show the plane and region of the brain in section. Scale bar = 200 μm in A,C–E; 50 μm in B; 20 μm in B.1,C.1,D.1,E.1.

cord that were MAG positive (Fig. 6D), mirroring the staining patterns of Nogo-A and NgR.

## Expression of Nogo-A, NgR, and MAG in Embryonic Axolotl CNS

Because MAF expression was widespread in the uninjured CNS and during regeneration, we examined Nogo-A, NgR, and MAG expression during development at a time when the spinal cord makes connections to peripheral targets (stage-45; hatching) (Nieuwenhuys et al., 1998). Immunohistochemical analysis showed expression of Nogo-A, NgR, and MAG in embryonic cord in white matter, gray matter neurons, and ependymal cells surrounding the central canal (Fig. 7A–I.1). Expression of all three proteins was also detected in the lens, retina (Fig. 7J–K,N–O,R–S), and forebrain neurons (Fig. 7L–M,L.1,P–Q,P.1). RT-PCR analysis corroborated these data, showing expression of *nogo-a* from stage-36 embryos to 2-month-old larvae (Fig. 7W). Whole-mount in situ hybridization spatially localized *nogo-a* mRNA in stage 36 and 38 embryos (Fig. 7X) to the developing brain, spinal cord, eye (Fig. 7X), and somites, mirroring where Nogo-A was expressed in adult tissues.

## Co-expression of Nogo-A and Sox2 in Developing and Injured Spinal Cord

Ependymal cells lining the central canal of the axolotl spinal cord are thought to provide neural progenitors during regeneration (Chernoff et al., 2003; McHedlishvili et al., 2012). To determine if Nogo-A is expressed in ependymal cells, we tested for colocalization of Nogo-A and Sox2, which is expressed in neural stem/progenitor cells across vertebrates (Graham et al., 2003; Ferri et al., 2004). Colocalization in ependymal cells was demonstrated in stage-40 embryos (Fig. 8A–D); however, Nogo-A did not colocalize with Sox2 in white matter. In adult uninjured cords, a few cells were $Sox2^+$ around the ependyma, although none of them colocalized with Nogo-A (Fig. 8G). Of interest, we found that many cells co-expressed Nogo-A and Sox2 in the gray matter of the adult injured cord (Fig. 8E,E.1). Similar to Nogo-A, we found NgR and Sox2 colocalization in the gray matter of 3 dpi cords (Fig. 8F,F.1). However, the number of $Nogo\text{-}A^+/Sox2^+$ cells (approximately 22% of cells) was higher than the $NgR^+/Sox2^+$ cells (approximately 10% of cells) at 3 dpi (Supp. Fig. S5). Furthermore, Sox2 expression was found both in glial and neuronal populations identified by using GFAP and NeuN, respectively (Fig. 8H–J). We also observed colocalized Sox2 expression with GFAP (Fig. 8H–J) in adjacent sections of Nogo-A/Sox2 and NgR/Sox2 stained sections. We found that some of the $Nogo\text{-}A^+/Sox2^+$ and $NgR^+/Sox2^+$ cells also stained positively for GFAP, with several cells displaying radial glial morphology (Fig. 8H,I,H.1,H.2,I.1). Radial morphology was not present in all the $GFAP^+/Sox2^+$ cells possibly because GFAP positive radial glia may lose their radial morphology after injury (Chernoff, 1996). Alternatively, these $GFAP^+/Sox2^+$ aggregated cells may be ependymal cells that

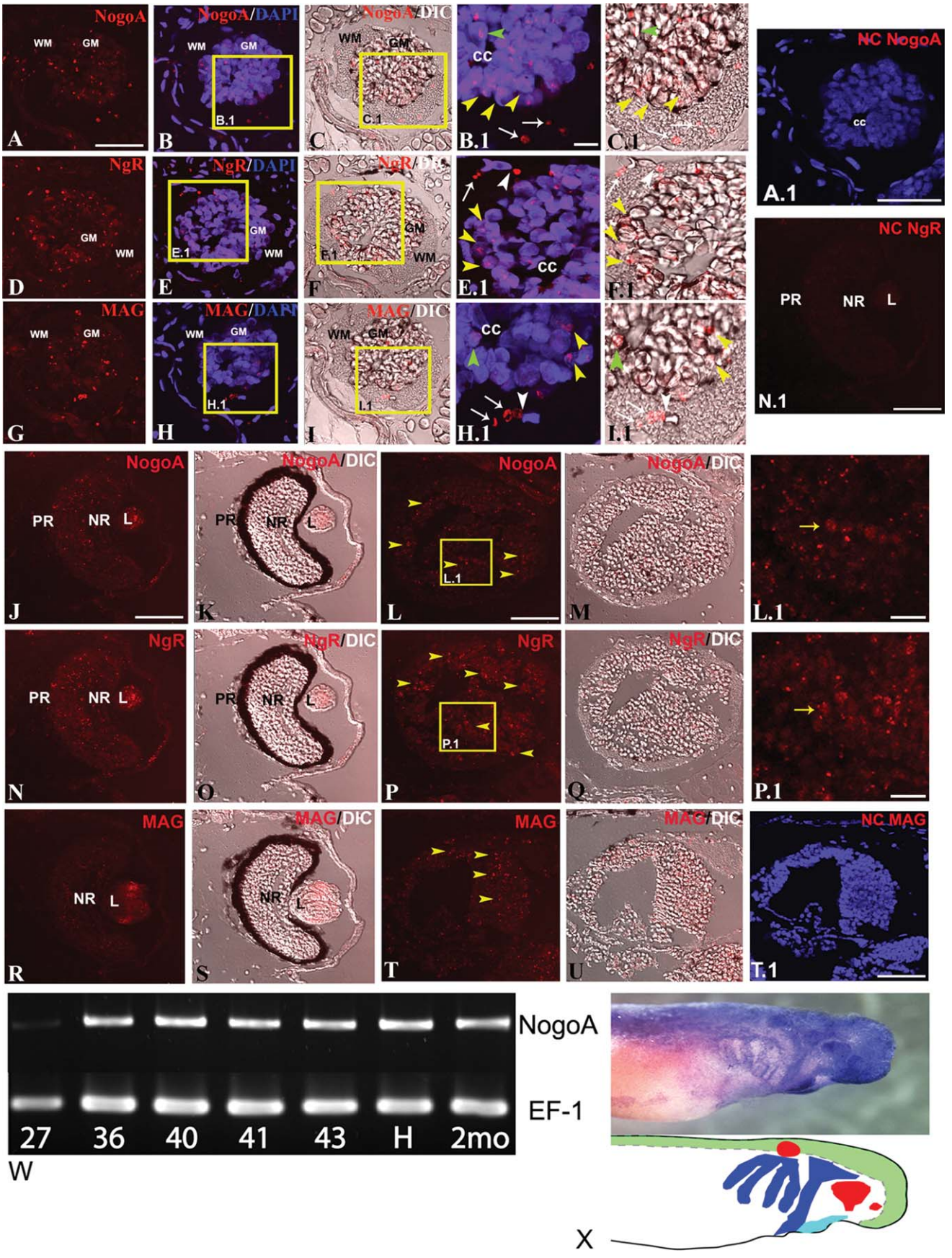
NogoA
NogoA/DAPI
NogoA/DIC
NC NogoA
NgR
NgR/DAPI
NgR/DIC
NC NgR
MAG
MAG/DAPI
MAG/DIC
NC MAG
WM
GM
CC
PR
NR
L
27
36
40
41
43
H
2mo
EF-1

Fig. 7.

migrate towards the lesion, as was shown in injured *X. laevis* spinal cords (Gaete et al., 2012). Therefore, a sub-population of both neurons and ependymal cells were Sox2 positive (Fig. 8H–J,H.1,H.2,I.1,J.1). Of interest, a few sub-pial cells were also Nogo-A$^+$/Sox2$^+$ and NgR$^+$/Sox2$^+$ (Fig. 8E.3,F.2).

## DISCUSSION

### Identification and Expression of Nogo-A, NgR, and MAG in Adulthood and After Injury

In contrast to mammals, transected spinal cord axons regenerate successfully following injury in the axolotl (O'Hara et al., 1992; Chernoff, 1996; Chernoff et al., 2003). Here, we studied axon regrowth using a transection injury model because it produces two clear stumps without spared axons. Moreover, in contrast to tail amputation (e.g., McHedlishvili et al., 2007), spinal cord transection is a less complicated injury model because axons can be studied with less interference from other regenerating tissues. Finally, transection injuries (as well as crush injuries) more closely mimic SCIs that occur in mammals and, therefore, are better models for mammalian SCI. Both our histological analysis and time course analysis of RT-97 protein expression revealed reconnected axons in the injury epicenter following transection injury, thus confirming axon regrowth in the axolotl. We also showed that the axolotl expresses MAF genes and corresponding receptors that are known to have inhibitory properties on axon regeneration in mammals. The presence of MAFs in zebrafish and urodeles, animals capable of spinal cord regeneration throughout their life, indicates an early vertebrate origin for MAFs that are permissive for regeneration. We propose it is not the presence or absence of MAFs that explain regenerative ability. Indeed, deletion of all three Nogo isoforms, MAG, and OMGP does not increase axon regeneration following SCI in mice (Lee et al., 2010).

The expression of Nogo-A, NgR, and MAG in the axolotl CNS, before and after injury, was mainly in neurons, axons and a few white matter cells. This suggests that MAFs are likely playing roles both in the uninjured and injured nervous system. Indeed, Nogo-A is known to function in the uninjured mammalian CNS as a stabilizer of axonal and synaptic connectivity (Park et al., 2010; Schwab, 2010; Pernet and Schwab, 2012). Furthermore, the other MAFs play redundant (Zheng et al., 2006; Liu et al., 2006) and synergistic roles (Cafferty et al., 2010) in this regard.

Our study shows that Nogo-A, MAG, and NgR expression is broader than white matter. Most importantly, we observed that many NeuN$^+$ neurons express Nogo-A, as do some GFAP$^+$ glial cells located in the subependyma. We found both GFAP$^+$/Nogo-A$^+$ and GFAP$^+$/NgR$^+$ cells largely in sub-ependyma, with very few in the ependyma. Both of these cell types may or may not show radial glial morphology because loss of ependymal glial morphology is a characteristic feature of urodele and fish cord after injury (Chernoff, 1996; Hui et al., 2010). The predominant cell type expressing Nogo-A and NgR in both the brain and spinal cord was neurons. Similar neuronal patterns of Nogo-A and NgR expression have been observed in the embryonic mammalian CNS (Huber et al., 2002). These data suggest that Nogo-A expression is correlated with the high regenerative capacity of neurons and may have a role in synaptic plasticity, as suggested by others (Huber et al., 2002; Hunt et al., 2002; Schwab, 2010; Peng et al., 2011). In contrast to mammals, the expression of axolotl MAFs is not consistent with an axonal inhibitory role after SCI; expression in adult axolotl is associated primarily with gray matter whereas in mammals Nogo-A is primarily localized to oligodendrocytes (Chen et al., 2000). Analysis of effects of IN-1 antibody generated against NI-220/250 peptide on oligodendrocyte culture in rodent further confirm the specific role of Nogo-A in these cells. Furthermore, the early developing chick CNS (E3 stage) expresses Nogo-A primarily in neurons, followed by high expression in axons at or near E12 stage. Nogo-A expression is correlated with generation of motor neurons and axonal outgrowth in early development well before the expression in O4 positive oligodendrocytes

**Fig. 7.** Expression of Nogo-A, Nogo receptor (NgR), and myelin associated glycoprotein (MAG) in developing axolotl CNS. Immunolocalization of Nogo-A (A–C,J–M), NgR (D–F,N–Q) and MAG (G–I,R–U) in developing spinal cord (A–I), retina (J,K,N,O,R,S) and forebrain (L,M,P,Q,T,U) of stage-45 axolotl embryos. **A–C:** Cross-section of spinal cord showing Nogo-A positive staining in white matter (WM) and gray matter (GM). **B.1,C.1:** Respective higher magnifications of sections B and C shows Nogo-A staining in neurons (yellow arrowhead), axons (white arrow) and ependymal cells (green arrowhead) around the central canal (cc). **A.1:** Spinal cord section stained without Nogo-A primary antibody; a negative control (NC). **D–F:** Cross-section of spinal cord showing NgR staining in gray matter (GM) and white matter (WM). **E.1,F.1:** Higher magnification of sections E and F shows positive staining in neurons (yellow arrowhead) and axons (white arrow). **G–I:** Cross-section of spinal cord showing MAG staining in white (WM) and gray matter (GM). **H.1,I.1:** Higher magnification of sections H and I shows positive staining in neurons (yellow arrowhead), axons (white arrow) and ependymal cell (green arrowhead). **J,K:** A transverse section of the eye shows Nogo-A staining in lens (L), neural retina (NR) and pigmented retina (PR). **L,M:** A coronal section of forebrain shows many Nogo-A positive neuronal cells (yellow arrowhead). **L.1:** Higher magnification of same section in L shows Nogo-A staining in neurons (yellow arrow), colocalized with NgR as the two antibody staining was done in adjacent section as represented in P.1. **N,O:** A transverse section of eye showing NgR staining in lens (L), neural retina (NR) and pigmented retina (PR). **N.1:** Eye section stained without NgR primary antibody; a negative control (NC). **P,Q:** A coronal section of forebrain that was adjacent to the section presented in L and M shows many NgR positive neuronal cells (yellow arrowhead). **P.1:** Higher magnification of the same section (P) shows staining in neurons (yellow arrow). **R,S:** A transverse section of eye showing MAG staining in lens (L) and neural retina (NR). Note that staining of MAG is weaker than Nogo-A and NgR. **T,U:** A transverse section of forebrain showing MAG positive cells (yellow arrowhead) in gray matter. **T.1**: Forebrain section stained without MAG primary antibody; a negative control (NC). **V:** Transverse section of spinal cord from a stage-45 axolotl embryo stained without Nogo-A primary antibody. **W:** Expression of *rtn4* (*nogo-A*) and *ef1α* mRNA during development. Axolotl embryo stages follow Beetshcen and Gautier's classification. **X:** Whole-mount in situ hybridization of stage-38 embryos using an antisense probe against *axNogo-A*. Purple staining shows the locations of *nogo-A* mRNA. The schematic diagram shows where *nogo-A* staining was observed in the embryo. Green: central nervous system; Red: sensory placodes including olfactory, visual and otic placodes; Blue: neural crest migration paths. "cc" denotes the central canal. Scale bar = 50 μm in A–I,J–U,A.1,N.1,T.1, 20 μm in B.1,C.1,E.1,F.1,H.1,I.1, 10 μm in L.1,P.1.

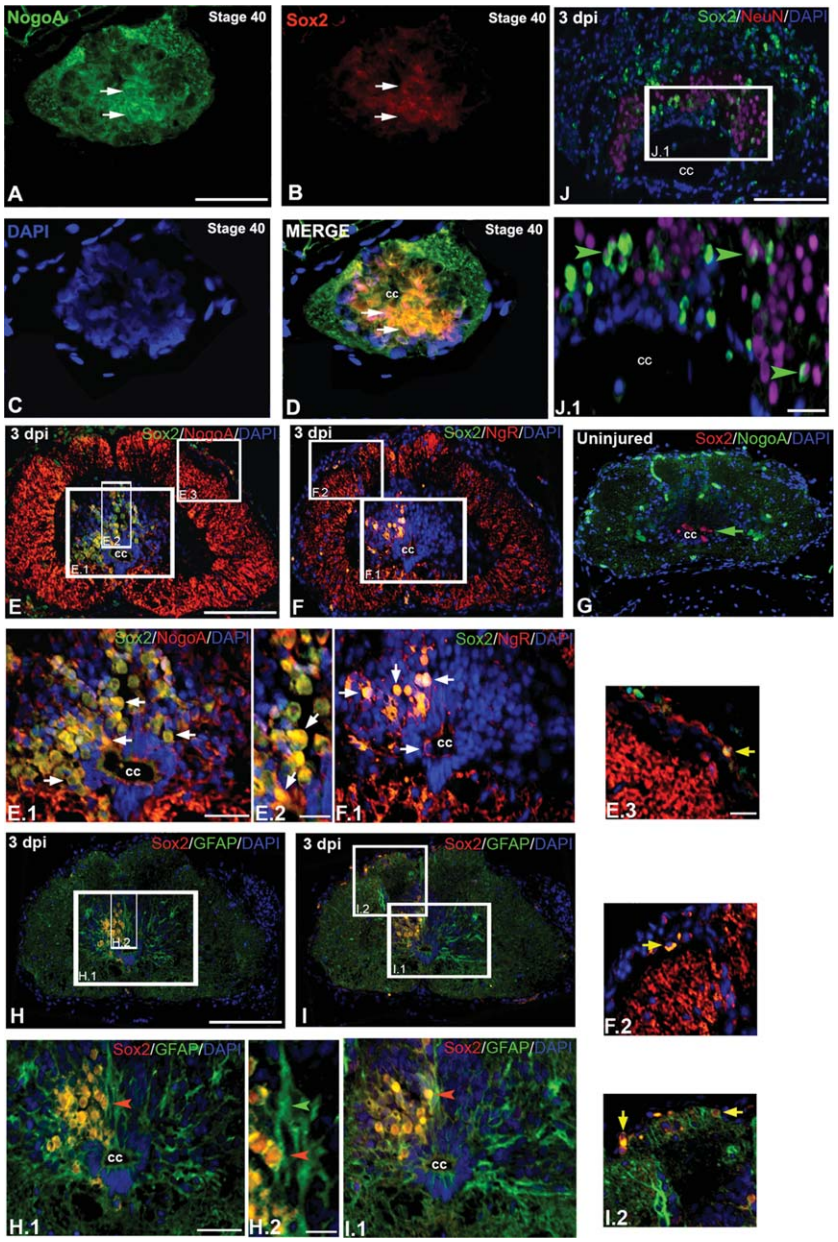


**Fig. 8.** Immunohistochemical localization of Nogo-A and Sox2 in stage-40 axolotl embryonic spinal cord, and adult uninjured and injured cord. **A–D:** Transverse sections of stage-40 embryonic cord shows Nogo-A and Sox2 colocalized cells (white arrow) in the gray matter. **E:** A transverse section of 3 days post-injury (dpi) cord shows many Nogo-A and Sox2 colocalized cells. **E.1,E.2:** The same section (E) in higher magnification shows colocalized cells (white arrow) in the gray matter near the injury epicenter. **E.3:** The same section (E) in higher magnification shows a sub-pial cell is both Nogo-A and Sox2 positive (yellow arrows). **F:** A transverse section of 3 dpi cord shows many Nogo receptor (NgR) and Sox2 colocalized cells. **F.1:** The same section (F) in higher magnification showing NgR and Sox2 positive cells (white arrows) in the gray matter near the injury epicenter. **F.2:** Note that a sub-pial cell is also NgR and Sox2 positive (yellow arrows) in the higher magnification of section F. **G:** Transverse section of uninjured cord stained with both Nogo-A and Sox2 showing very few cells are Sox2 positive (green arrow). **H,I:** Transverse sections of 3 dpi cord. Sections H and I were taken from positions adjacent to E and F, respectively, and stained with Sox2 and glial fibrillary acidic protein (GFAP). **H.1,H.2,I.1:** Higher magnifications of the boxed areas of H and I show colocalized Sox2 and GFAP positive cells (H.1 and I.1, red arrowheads) in the gray matter of injured cord. The section in H.2 shows a Sox2 and GFAP positive cell where Sox2 stains the nucleus (red arrowhead) and GFAP stains fibril cytoplasm (green arrowhead). **I.2:** The same section (I) in higher magnification shows few sub-pial cells are both GFAP and Sox2 positive (yellow arrows). **J:** A transverse section of a 3dpi cord at the stump level, stained with Sox2 and NeuN. **J.1:** Higher magnification of the same section (J) shows few colocalized Sox2 and NeuN positive cells (green arrowheads) in the gray matter. "cc" denotes the central canal. Scale bar = 100 μm in E–J, 50 μm in A–D, 20 μm in E.1,F.1,H.1,I.1,J.1,E.3,F.2,I.2, 10 μm in E.2,H.2.

and, thus, suggesting a role in neuronal and axon development (O'Neill et al., 2004). A population of Nogo-A positive cells also expresses NgR as shown by us (Supp. Fig. S6) and others (Huber et al., 2002; O'Neill et al., 2004); in our study, co-expression was observed in both injured and uninjured adult axolotl cord. This may indicate a role for Nogo-A/NgR signaling in developing and regenerating CNS.

## Expression of Nogo-A, NgR, and MAG During CNS Development

Our study is the first to show the expression of myelinating inhibitory proteins and their receptors in axolotl during embryonic life and adulthood. We localized Nogo-A, NgR, and MAG in the developing axolotl CNS, including the brain, spinal cord, and eye. In the stage-45 embryo cortex and spinal cord, neurons (and associated axons) and ependymal cells express all three molecules and many express both NgR and Nogo-A. The developing eye also showed expression of Nogo-A, NgR, and MAG in retina and lens. Interestingly, Nogo-A and NgR are expressed during mammalian CNS development in both radial glia and in retinal ganglion cells (O'Neill et al., 2004; Wang et al., 2008, 2010; Petit et al., 2011). In developing chick and human spinal cord, both Nogo-A and NgR are expressed early during development and their expression levels remain unchanged after injury at stages permissive for regeneration (O'Neill et al., 2004). This observation indicates that Nogo-A likely has an important role in development, possibly to direct axons to their proper targets. In zebrafish, expression of NgR during development is similar to mammals and implicated in axonal outgrowth and guidance of PNS projections (Brosamle and Halpern, 2009). Our results support findings observed in other vertebrates, suggesting that Nogo-A and NgR expression is related to neuronal and synaptic plasticity (Huber et al., 2002; Hunt et al., 2003; Meier et al., 2003; Richard et al., 2005; Schwab, 2010). Moreover, MAFs are associated with both development and regeneration of

CNS, suggesting that these may have similar roles and, thus, create an embryonic environment in the adult CNS.

### Nogo-A and NgR Are Expressed in Neural Progenitors Both in Adult Regenerating and in Developing Spinal Cord

The transcription factor *sox2* is considered to be a pan-neural marker during development (Wegner, 1999), because it is widely expressed in the prospective neuroectoderm and early neural tube in several species including chick, mouse, and *X. laevis*. At later stages, expression becomes restricted to proliferating neuroepithelial cells of the ventricular layer. Mammalian Sox2 is expressed in neural progenitor cells throughout the developing and adult CNS and is implicated in the maintenance of the neural progenitor state; its loss of function triggers cell cycle exit followed by neuronal differentiation (Hutton and Pevny, 2011). We observed that Sox2 is expressed in the uninjured adult axolotl spinal cord predominantly in gray matter, although at a much lower level when compared with the regenerating spinal cord. During regeneration, Sox2 positive cells were present in GFAP expressing sub-ependyma. Similar up-regulation of Sox2 in the ependyma and sub-ependyma of the regenerating cord was documented in *Pleurodeles* (Ferretti et al., 2001) and *X. laevis* (Gaete et al., 2012) after tail amputation. Sox2 positive neural stem cell-like progenitors are indeed present in the adult zebrafish cord and their number increases after injury (our unpublished observation). Furthermore, adult zebrafish have telencephalic ventricular cells of the brain that also express Sox2 and are neurogenic (Adolf et al., 2006).

In the adult mammalian spinal cord, the main progenitor cells are localized in the ependymal and subependymal layers of the central canal ventricular zone. These cells have the characteristics of neural stem cells (NSC) as they express markers such as Sox2, vimentin, GFAP, nestin, and BLBP (Petit et al., 2011). In the regenerating urodele cord, there are many migrating progenitors and similar to the mammalian cord, expression of NSC markers has also been observed (O'Hara et al., 1992; Ferretti et al., 2001; Walder et al., 2003). The colocalization of Nogo-A and NgR with Sox2 both in the developing and regenerating axolotl cord confirms that these molecules are expressed in neural progenitors and may participate in spinal cord repair process. This conclusion is supported by reports from other species showing that Sox2 positive progenitors contribute to regeneration (Lin et al., 2009; Arnold et al., 2011; Gaete et al., 2012). A small percentage of sub-pial white matter cells were also positive for both Sox2 and Nogo-A, or Sox2 and NgR. Sub-pial neurogenesis is a known process in mouse and zebrafish CNS (Mueller and Wullimann, 2002; Li et al., 2009; Hui et al., 2010). It is of interest to characterize these sub-pial cells to address whether they contribute to spinal cord regeneration or not in the urodele.

## EXPERIMENTAL PROCEDURES

### Axolotl Maintenance

Albino or white axolotls (*Ambystoma mexicanum*) were either purchased from the Ambystoma Genetic Stock Center (University of Kentucky, Lexington, KY) or spawned at the animal house facility of University of Calcutta. Larvae were maintained at 20–22°C in 40% Holtfreter's solution. Animals measuring 6–8 cm snout to cloaca were used to inflict spinal cord injury.

### Surgical Procedures for Inflicting Spinal Cord Injury to Axolotl

Animal housing and experiments were approved by the University of Kentucky, University of Florida, and University of Calcutta Committees on Animal Care and Use. Animals were imported from the Ambystoma Genetic Stock Center at the University of Kentucky as approved by CITES permission to Dr. Sukla Ghosh, University of Calcutta. Animals were anesthetized for 5 min in 0.02% buffered benzocaine (Sigma, St. Louis, MO) and spinal cord transection was performed near the hind limb level. After surgery, the wounds were closed and animals were allowed to recover. At least 5 spinal cord transected animals were examined for each time point and injury response was further characterized by histological analysis. Tissues were collected at different time points following intra-cardial perfusion with phosphate buffered saline and 4% paraformaldehyde. The tissues were further fixed in 4% paraformaldehyde overnight, processed and embedded in paraplast or paraffin.

### RNA Extraction and RT-PCR

Axolotls measuring 8–10 cm snout to cloaca were anesthetized and spinal cord tissue was collected 1 mm anterior and posterior to the transection site and snaps frozen in liquid nitrogen. RNA isolation was performed using Rneasy columns (Qiagen) and quantified using an Epoch spectrophotometer (BioTek). cDNA was produced using 1 μg total RNA and the iScript cDNA synthesis kit using Oligo(dT) 20 primers (Bio-Rad). Templates for PCR included cDNA corresponding to 10 ng of total RNA and 500 nM forward and reverse primers. PCR primers were as follows: *nogo-A* forward 5′-TGA TGG AAA AAC TGG GGA GA-3′ and reverse 5′-GGG GAT GTA CGG AGT CTC AA-3′; *rtn4r* forward 5′-GCA CTC TGG CAG GAA AAG AC-3′ and reverse 5′-TGG CAG CAA CAA ACT GAG AC-3′; *ef-1α* forward 5′-AAC ATC GTG GTC ATC GGC CAT-3′ and reverse 5′-GGA GGT GCC AGT GAT CAT GTT-3′. PCR parameters for *nogo-A* and rtn4r were 28 cycles of 94°C for 45 sec, 55°C for 45 sec, 72°C for 45 sec, and 24 cycles using the same parameters for *ef-1α*. Five microliters of PCR product was analyzed on a 1% agarose gel and visualized using a FluorChem E Imaging system (Cell Biosystems).

### In Situ Hybridization

The 991 bp PCR product for nogo-A was cloned into a Promega pGEM-T vector by the A-tailing procedure, and Nogo-A digoxygenin-labeled RNA probe was produced using M13

forward and reverse primers and T7 or SP6 polymerase as described in the Roche DIG-RNA labeling manual. Tissue samples were fixed in 4% paraformaldehyde/1×PBS overnight, cryoprotected by immersion in 10% sucrose/1×PBS and 20% sucrose/1×PBS for 1 hr each, followed by immersion in 30% sucrose/1×PBS for 3 hr to overnight. Tissues were then mounted in OCT medium, sectioned at 16 μm, and stored at −80°C. Hybridization was carried out at 55°C overnight, washed, visualized with NBT/BCIP, and sections were mounted in Permount. Whole-mount in situ hybridization was carried out according to (Monaghan and Maden, 2012), which was based upon a protocol provided by David Parichy (University of Washington, USA). Multiple embryos were observed to confirm the expression patterns, and tracing of expression patterns was performed using an Intuos4 pen tablet (Wacom) and processed using Adobe Illustrator 5.

### Mapping of axNogo-A, Sequence Alignment, and Analysis

Axolotl Nogo-A sequences were deposited in GenBank (accession no. JX276741). Mapping of axNogo was performed according to (Smith et al., 2005) using the following primers: forward 5′-GAA GAC GAT GAA ACG ACT GAG AG-3′, 5′-CCG CAG CGC CAG GTG ATG GTC GAG GAA-3′, and reverse 5′-GGC TTC TTC CTC TCC TCA AAA G-3′. *Rattus norvegicus*, *Mus domesticus*, *Homo sapiens*, *Gallus gallus*, and *Xenopus laevis* Nogo-A sequences are obtained from NCBI (NP_114019, NP_918943, NP_065393, NP_989697, and AAQ82646, respectively). Sequence alignments were performed using CLUSTALW and regions of sequence similarity were shaded using BOXSHADE. Hydrophobic regions were predicted using Tmpred, TMHMM (Krogh et al., 2001).

### Histology and Immunohistochemistry

For histology of spinal cord and brain, tissues were embedded either in paraffin, in a mixture of poly-ethylene glycol (PEG) and hexadecanol (9:1, Sigma), or in O.C.T. compound (Leica, Germany) and sectioned at 5–7 μm. Sections were stained either with Mallory's trichrome stain (Humason, 1979) or with luxol fast blue & cresyl violet (Kluver and Barrera, 1953). Immunohistochemistry was performed either in paraplast or paraffin sections of 10 μm as described by Hui et al. (2010). The following primary antibodies were used: NgR (1:100) polyclonal antibody (Santa Cruz Biotechnology, USA), Nogo-A (1:50) polyclonal antibody (Santa Cruz Biotechnology, USA), MAG (1:100) polyclonal antibody (Santa Cruz Biotechnology, USA), NeuN (1:400, monoclonal antibody from Chemicon, USA), Sox-2 (1:200, Abcam, USA), GFAP (1: 500, DAKO, USA) and RT-97 (1:3,000) to stain neurofilament associated protein (gift from Dr. Ron Meyer, USA). Details of reactivity for the following antibodies have been described: NeuN (McHedlishvili et al., 2012), GFAP (O'Hara et al., 1992), RT-97 (Hunter et al., 1991), and Sox2 (Gaete et al., 2012). Following antibody incubation, sections were given several washes with either PBS Tween-20 or 0.03% Triton X-100. Sections were then treated with the appropriate dilution of either anti-mouse, anti-goat, or anti-rabbit secondary antibodies coupled to fluorescein isothiocyanate (FITC) or Rhodamine (Jackson laboratory, USA), counter stained with DAPI (4′,6-diamidine-2-phenylidole-dihydrochloride; Roche), mounted with Vectashield and visualized using either an Olympus Fluorescence microscope (Model- BX51) equipped with digital cooled CCD Camera (Model-Evolution VF Mono) and ImagePro-Express software, or a Zeiss 510 meta confocal microscope.

### Immunoblotting

Axolotl tail blastema was collected 7 and 15 days after amputation along with the control, unamputated tails. Tissues were prepared in extraction buffer (37.5 mM Tris, 75 mM NaCl, 0.5% Triton X-100, protease inhibitor cocktail) and then the resulting tissue lysates were subjected to 7.5% sodium dodecyl sulfate polyacrylamide gel electrophoresis (SDS-PAGE). After electrophoresis, proteins were transferred onto nitrocellulose membranes and subjected to Western blotting. The Western blots were developed with anti-NgR (1:1,000; Santa Cruz Biotechnology, USA), anti-Nogo-A (1:500; Santa Cruz Biotechnology, USA), and anti-MAG (1:1,000; Santa Cruz Biotechnology, USA) antibody followed by anti-goat and anti-rabbit alkaline phosphatase coupled secondary antibody (1:1,000; Jackson laboratory, USA). Protein bands were visualized using NBT/BCIP as substrate. PageRuler Broad Range Protein Ladder (Thermo Scientific, USA) was used as a standard molecular weight marker.

## ACKNOWLEDGMENTS

This work was supported by the Department of Science and technology, Ministry of Science and Technology, Govt. of India and partly by Department of Biotechnology, Ministry of Science and Technology, Govt. of India to Sukla Ghosh. S. P. Hui is recipient of a senior research fellowship from the Council of Scientific and Industrial Research, Govt. of India. The project also used resources from the Ambystoma Genetic Stock Center, which is funded by grant DBI-0951484 from the National Science Foundation. This work was also supported by a grant from the Kentucky Spinal Cord and Brain Injury Research Trust awarded to S.R. Voss. S. P. Hui performed all histology, Western blotting and immunohistochemistry. J. R. Monaghan performed mRNA expression analysis. S. P. Hui, J. R. Monaghan, S. R. Voss, and S. Ghosh designed the experiments. S. P. Hui and S. Ghosh wrote the manuscript.

## REFERENCES

Adolf B, Chapouton P, Lam CS, Topp S, Tannhauser B, Strahle U, Gotz M, Bally-Cuif L. 2006. Conserved and acquired features of adult neurogenesis in the zebrafish telencephalon. Dev Biol 295:278–293.

Ankerhold RC, Leppert A, Bastmeyer M, Stuermer CA. 1998. E587 antigen is upregulated by gold fish oligodendrocytes after optic nerve lesion and supports retinal axon regeneration. Glia 23: 257–270.

Arnold K, Sarkar A, Yram MA, Polo JM, Bronson R, Sengupta S, Seandel M, Geijsen N, Hochedlinger K. 2011.

Sox2(+) adult stem and progenitor cells are important for tissue regeneration and survival of mice. Cell Stem Cell 9:317–329.

Bastmeyer M, Beckman M, Schwab ME, Stuermer CA. 1991. Growth of regenerating goldfish axons is inhibited by rat oligodendrocytes and CNS myelin but not by goldfish optic nerve tract oligodendrocyte-like cells and fish CNS myelin. J Neurosci 11:626–640.

Berry M. 1982. Post injury myelin breakdown products inhibit axonal growth: a hypothesis to explain the failure of axonal regeneration in the mammalian central nervous system. Bibl Anat 23: 1–11.

Bradford Y, Conlin T, Dunn N, Fashena D, Frazer K, Howe DG, Knight J, Mani P, Martin R, Moxon SA, Paddock H, Pich C, Ramachandran S, Ruef BJ, Ruzicka L, Bauer Schaper H, Schaper K, Shao X, Singer A, Sprague J, Sprunger B, Van Slyke C, Westerfield M. 2011. ZFIN: enhancements and updates to the Zebrafish Model Organism Database. Nucleic Acids Res 39: D822–D829.

Brosamle C, Halpern ME. 2009. Nogo-Nogo receptor signalling in PNS axon outgrowth and pathfinding. Mol Cell Neurosci 40:401–409.

Buchli AD, Schwab ME. 2005. Inhibition of Nogo: a key strategy to increase regeneration, plasticity and functional recovery of the lesioned central nervous system. Ann Med 37:556–567.

Burridge K, Wennerberg K. 2004. Rho and Rac take center stage. Cell 116:167–179.

Cafferty WB, Duffy P, Huebner E, Strittmatter SM. 2010. MAG and OMgp synergize with Nogo-A to restrict axonal growth and neurological recovery after spinal cord trauma. J Neurosci 30: 6825–6837.

Caroni P, Schwab ME. 1988. Two membrane protein fractions from rat central myelin with inhibitory properties for neurite outgrowth. J Cell Biol 106:1281–1288.

Chen MS, Huber AB, Van Der Haar ME, Frank M, Schnell L, Spillmann AA, Christ F, Schwab ME. 2000. Nogo-A is a myelin-associated neurite outgrowth inhibitor and an antigen for monoclonal antibody IN-1. Nature 403:434–439.

Chernoff EA. 1996. Spinal cord regeneration: a phenomenon unique to urodeles? Int J Dev Biol 40:823–831.

Chernoff EA, Stocum DL, Nye HL, Cameron JA. 2003. Urodele spinal cord regeneration and related processes. Dev Dyn 226:295–307.

Diekmann H, Klinger M, Oertle T, Heinz D, Pogoda HM, Schwab ME, Stuermer CA. 2005. Analysis of the reticulon gene family demonstrates the absence of the neurite growth inhibitor Nogo-A in fish. Mol Biol Evol 22:1635–1648.

Domeniconi M, Cao Z, Spencer T, Sivasankaran R, Wang K, Nikulina E, Kimura N, Cai H, Deng K, Gao Y, He Z, Filbin M. 2002. Myelin associated glycoprotein interacts with Nogo-66 receptor to inhibit neurite outgrowth. Neuron 35:283–290.

Ferretti P, Zhang F, Santos-Ruiz L, Clarke JDW. 2001. FGF signalling and blastema growth during amphibian tail regeneration. Int J Dev Biol 45:S127–S128.

Ferri AL, Cavallaro M, Braida D, Di Cristofano A, Canta A, Vezzani A, Ottolenghi S, Pandolfi PP, Sala M, DeBiasi S, Nicolis SK. 2004. Sox2 deficiency causes neurodegeneration and impaired neurogenesis in the adult mouse brain. Development 131:3805–3819.

Fournier AE, Grandpre T, Strittmatter SM. 2001. Identification of a receptor mediating Nogo-66 inhibition of axonal regeneration. Nature 409:341–346.

Freund P, Schmidlin E, Wannier T, Bloch J, Mir A, Schwab ME, Rouiller EM. 2006. Nogo-A specific antibody treatment enhances sproutin and functional recovery after cervical lesion in adult primates. Nat Med 12:790–792.

Gaete M, Munoz R, Sanchez N, Tampe R, Moreno M, Contreras EG, Lee-Liu D, Larrain J. 2012. Spinal cord regeneration in Xenopus tadpoles proceeds through activation of Sox2 positive cells. Neural Dev 7:13.

Graham V, Khudyakov J, Ellis P, Pevny L. 2003. SOX2 functions to maintain neural progenitor identity. Neuron 39:749–765.

Grandpre T, Nakamura F, Vartanian T, Strittmatter SM. 2000. Identification of the Nogo inhibitor of axon regeneration as a reticulon protein. Nature 403:439–444.

Huber AB, Weinman O, Brosamle C, Oertle T, Schwab ME. 2002. Patterns of Nogo mRNA and protein expression in the developing and adult rat and after CNS lesions. J Neurosci 22:3553–3567.

Hui SP, Dutta A, Ghosh S. 2010. Cellular response after crush injury in adult zebrafish spinal cord. Dev Dyn 239:2962–2979.

Humason GL. 1979. Animal Tissue techniques. New York: WH Freeman & Co.

Hunt D, Coffin RS, Anderson PN. 2002. The Nogo receptor, its ligands and axonal regeneration in the spinal cord; a review. J Neurocytol 31:93–120.

Hunt D, Coffin RS, Prinjha RK, Campbell G, Anderson PN. 2003. Nogo-A expression in the intact and injured nervous system. Mol Cell Neurosci 24:1083–1102.

Hunter K, Maden M, Summerbell D, Eriksson U, Holder N. 1991. Retinoic acid stimulates neurite outgrowth in the amphibian spinal cord. Proc Natl Acad Sci U S A 88:3666–3670.

Hutton SR, Pevny LH. 2011. SOX2 expression levels distinguish between neural progenitor populations of the developing dorsal telencephalon. Dev Biol 352:40–47.

Klinger M, Taylor JS, Oertle T, Schwab ME, Steurmer CAO, Diekmann H. 2004. Identification of Nogo-66 receptor (NgR) and homologous genes in fish. Mol Biol Evol 21:76–85.

Kluver H, Barrera E. 1953. A method for the combined staining of cells and fibres in the nervous system. J Neuropath Exp Neurol 12:400–403.

Kottis V, Thibault P, Mikol D, Xiao ZC, Zhang R, Dergham P, Braun PE. 2002. Oligodendrocyte-myelin glycoprotein (OMgp) is an inhibitor of neurite outgrowth. J Neurochem 82:1566–1569.

Krogh A, Larsson B, von Heijne G, Sonnhammer EL. 2001. Predicting transmembrane protein topology with a hidden Markov model: application to complete genomes. J Mol Biol 305:567–580.

Lang DM, Rubin BP, Schwab ME, Stuermer CA. 1995. CNS myelin and oligodendrocytes of the Xenopus spinal cord-but not optic nerve-are nonpermissive for axon growth. J Neurosci 15:99–109.

Lee JK, Geoffroy CG, Chan AF, Tolentino KE, Crawford MJ, Leal MA, Kang B, Zheng B. 2010. Assessing spinal axon regeneration and sprouting in Nogo-, MAG-, and OMgp-deficient mice. Neuron 66:663–670.

Li G, Kataoka H, Coughlin SR, Pleasure SJ. 2009. Identification of a transient subpial neurogenic zone in the developing dentate gyrus and its regulation by Cxcl12 and reelin signaling. Development 136:327–335.

Lin YP, Ouchi Y, Satoh S, Watanabe S. 2009. Sox2 plays a role in the induction of amacrine and Müller glial cells in mouse retinal progenitor cells. Invest Ophthalmol Vis Sci 50:68–74.

Liu BP, Fournier A, Grandpre T, Strittmatter SM. 2002. Myelin-associated glycoprotein as a functional ligand for the Nogo-66 receptor. Science 297:1190–1193.

Liu BP, Cafferty WB, Budel SO, Strittmatter SM. 2006. Extracellular regulators of axonal growth in the adult central nervous system. Phil Trans R Soc Lond B 361:1593–1610.

McGee AW, Strittmatter SM. 2003. The Nogo–66 receptor: focusing myelin inhibition of axon regeneration. Trends Neurosci 26:193–198.

McHedlishvili L, Epperlein HH, Telzerow A, Tanaka EM. 2007. A clonal analysis of neural progenitors during axolotl spinal cord regeneration reveals evidence for both spatially restricted and multipotent progenitors. Development 134: 2083–2093.

McKerracher L, David S, Jackson DL. 1994. Identification of myelin associated glycoprotein as a major myelin-derived inhibitor of neurite growth. Neuron 13:805–811.

McHedlishvili L, Mazurov V, Grassme KS, Goehler K, Robl B, Tazaki A, Roensch K, Duemmler A, Tanaka EM. 2012. Reconstitution of the central and peripheral nervous system during salamander tail regeneration. Proc Natl Acad Sci U S A 109:E2258–E2266.

Meier S, Brauer AU, Heimreich B, Schwab ME, Nitsch R, Savaskan NE. 2003. Molecular analysis of Nogo

expression in the hippocampus during development and following lesion and seizure. FASEB J 17:1153–1155.

Monaghan JR, Maden M. 2012. Visualization of retinoic acid signaling in transgenic axolotls during limb development and regeneration. Dev Biol 368:63–75.

Mueller T, Wullimann MF. 2002. BrdU-, neuroD (nrd)- and Hu-studies reveal unusual non-ventricular neurogenesis in the postembryonic zebrafish forebrain. Mech Dev 117:123–135.

Nieuwenhuys N, Donkelaar NH, Nicholson C. 1998. The central nervous system of vertebrates. Vol. 2, Chapter 18. Berlin: Springer-Verlag. p 1045–1115.

O'Hara CM, Egar MW, Chernoff EA. 1992. Reorganization of the ependyma during axolotl spinal cord regeneration: changes in intermediate filament and fibronectin expression. Dev Dyn 193:103–115.

O'Neill P, Whalley K, Ferretti P. 2004. Nogo and Nogo-66 receptor in human and chick: implications for development and regeneration. Dev Dyn 231:109–121.

Oertle T, Van Der Haar ME, Bandtlow CE, Robeva A, Burfeind P, Buss A, Huber AB, Simonen M, Schnell L, Bromsale C, Kaupmann K, Vallon R, Schwab ME. 2003. Nogo-A inhibits neurite outgrowth and cell spreading with three discrete regions. J Neurosci 23: 5393–5406.

Park KJ, Grosso CA, Aubert I, Kaplan DR, Miller FD. 2010. p75NTR-dependent, myelin-mediated axonal degeneration regulates neural connectivity in the adult brain. Nat Neurosci 13:559–566.

Peng X, Kim J, Zhou Z, Fink DJ, Mata M. 2011. Neuronal Nogo-A regulates glutamate receptor subunit expression in hippocampal neurons. J Neurochem 119:1183–1193.

Pernet V, Schwab ME. 2012. The role of Nogo–A in axonal plasticity, regrowth and repair. Cell Tissue Res 349:97–104.

Petit A, Sanders AD, Kennedy TE, Tetzlaff W, Glattfelder KJ, Dalley RA, Puchalski RB, Jones AR, Roskams AJ. 2011. Adult spinal cord radial glia display a unique progenitor phenotype. PLoS One 6:e24538.

Prinjha R, Moore SE, Vinson M, Blake S, Morrow R, Christie G, Michalovich D, Simmons DL, Walsh FS. 2000. Inhibitor of neurite outgrowth in humans. Nature 403:383–384.

Richard M, Giannetti N, Saucier D, Sacquet J, Jourdan F, Pellier-Monnin V. 2005. Neuronal expression of Nogo-A mRNA and protein during neurite outgrowth in the developing rat olfactory system. Eur J Neurosci 22:2145–2158.

Schwab ME. 2010. Functions of Nogo proteins and their receptors in the nervous system. Nat Rev Neurosci 11:799–811.

Schwab ME, Caroni P. 1988. Oligodendrocytes and CNS myelin are nonpermissive substrates for neurite outgrowth and fibroblast spreading in vitro. J Neurosci 8:2381–2393.

Shypitsyna A, Malaga-Trillo E, Reuter A, Stuermer CA. 2011. Origin of Nogo-A by domain shuffling in an early jawed vertebrate. Mol Biol Evol 28:1363–1370.

Smith JJ, Putta S, Walker JA, Kump DK, Samuels AK, Monaghan JR, Weisrock DW, Staben C, Voss SR. 2005. Sal-Site: integrating new and existing ambystomatid salamander research and informational resources. BMC Genomics 6:181.

Voss SR, Kump DK, Putta S, Pauly N, Reynolds A, Henry RJ, Basa S, Walker JA, Smith JJ. 2011. Origin of amphibian and avian chromosomes by fission, fusion, and retention of ancestral chromosomes. Genome Res 21:1306–1312.

Walder S, Zhang F, Ferretti P. 2003. Upregulation of neural stem cell markers suggests the occurrence of dedifferentiation in regenerating spinal cord. Dev Genes Evol 213:625–630.

Wang J, Chan CK, Taylor JS, Chan SO. 2008. Localization of Nogo and its receptor in the optic pathway of mouse embryos. J Neurosci Res 86:1721–1733.

Wang J, Wang L, Zhao H, Chan SO. 2010. Localization of an axon growth inhibitory molecule Nogo and its receptor in the spinal cord of mouse embryos. Brain Res 1306:8–17.

Wang KC, Koprivica V, Kim JA, Sivasankaran R, Guo Y, Neve RL, He Z. 2002. Oligodendrocyte-myelin glycoprotein is a Nogo receptor ligand that inhibits neurite outgrowth. Nature 417:941–944.

Wegner M. 1999. From head to toes: the multiple facets of Sox proteins. Nucleic Acids Res 27:1409–1420.

Zheng B, Lee JK, Xie F. 2006. Genetic mouse models for studying inhibitors of spinal axon regeneration. Trends Neurosci 29:640–646.